OFDM Opportunistic Relaying Under Joint Transmit/Receive I/Q Imbalance

Mohamed Mokhtar, *Student Member, IEEE*, Alexandros-Apostolos A. Boulogeorgos, *Student Member, IEEE*, George K. Karagiannidis, *Fellow, IEEE*, and Naofal Al-Dhahir, *Fellow, IEEE*

***Abstract*—We study the outage performance of orthogonal frequency-division multiplexing dual-hop opportunistic amplify-and-forward relaying in the presence of I/Q imbalance (IQI) in all nodes. We derive a closed-form expression for the end-to-end outage probability for the general case where each node suffers from a different IQI level and assuming that the distance between source and relay is not the same for all relays. Furthermore, we consider the more general case where there is a direct link between the source and the destination and we derive a closed-form expression for the end-to-end outage probability for both maximum-ratio and selection combining at the destination. To gain more insights, we analyze a special case where all relays lie on the perpendicular line midway between source and destination and all nodes experience the same IQI level. Our simulations show excellent match to the analytical results and both demonstrate that uncompensated IQI can be detrimental but it can also be effectively mitigated using a few opportunistic relays. In summary, the main contributions of this paper are analyzing the effect of IQI on the outage probability of an opportunistic relaying system and determining the number of relays needed to effectively mitigate uncompensated IQI.**

***Index Terms*—I/Q imbalance, amplify-and-forward, maximum ratio combining, selection combining, opportunistic relaying, OFDM.**

I. Introduction

WIRELESS networks with cooperative relaying have received considerable attention recently and have been adopted in wireless standards such as IEEE 802.16m [1] and LTE [2]. Among the most common relaying protocols is the so-called opportunistic relaying (OR) protocol which has been extensively analyzed in the literature [3]–[7], and is conceptually related to antenna selection in multi-antenna schemes [8]. In OR, the system is able to select the "best" relay, from a set of available candidate relays, to cooperate in order to avoid issues such as inter-node coordination, synchronization and interference with multiple active relays. A common selection strategy is to choose the relay that achieves the best end-to-end signal-to-noise-plus interference ratio (SINR).

The performance of relaying systems have been analyzed in several papers (see [9] and reference therein), assuming an ideal radio frequency (RF) front-end. However, in practice, the system performance is degraded by RF impairments, such as high-power amplifier (HPA) nonlinearity [10], in-phase and quadrature-phase (I/Q) imbalance (IQI), low-noise amplifier (LNA) nonlinearity, antenna coupling [11], phase noise (PN) and carrier frequency offset (CFO) [12], [13]. In particular, IQI represents the mismatch between analog components in the I and Q branches, which results from the limited accuracy of analog hardware and it can be either frequency-independent or frequency-dependent. Frequency-independent IQI occurs mainly due to non-ideal mixers and phase shifters and is constant over the whole signal bandwidth, while frequency-dependent IQI is due to I and Q low-pass filters mismatches. For orthogonal frequency-division multiplexing (OFDM) systems, IQI degrades the system performance severely due to image subcarrier interference [14]. In this paper, we will focus on studying the performance degradation due to frequency-independent IQI.

Scanning the open literature, the impact of PN on the performance of OFDM-based amplify-and-forward (AF) relay networks was investigated in [13] where it was shown that the use of an AF-relay becomes not beneficial, compared to a direct transmission, as the PN level exceeds a certain threshold. Furthermore, the outage performance for the AF relaying protocol was studied in [12] and [15]. Specifically, in [12] IQI was considered only at the destination and flat-fading links were assumed, while in [15] both the relay and the destination nodes suffer from IQI in the presence of frequency-selective fading links [16].

Cooperative communication closely mimics multiple input multiple output (MIMO) wireless systems [17], where the physical transceiver implementations were extensively investigated [18], [19]. In [18] the influence of transmitter (Tx) as well as receiver (Rx) IQI on the performance of multiple-antenna OFDM systems based on a direct-conversion RF front-end was studied. In [20], the authors analyzed the performance of MIMO-OFDM systems with independent PN sources at the transmit and receive RF front-end using zero-forcing detectors over frequency-selective Rayleigh fading channels.

A. Contributions

The contributions of this paper are as follows:

Manuscript received November 17, 2013; revised February 10, 2014. The editor coordinating the review of this paper and approving it for publication was R. Dinis.

M. Mokhtar and N. Al-Dhahir are with the University of Texas at Dallas, USA (e-mail: {m.mokhtar, aldhahir}@utdallas.edu). Their work was made possible by NPRP grant # NPRP 09-062-2-035 from the Qatar National Research Fund (a member of Qatar Foundation). The statements made herein are solely the responsibility of the authors.

A. Boulogeorgos and G. K. Karagiannidis are with Aristotle University of Thessaloniki, Greece (e-mail: {ampoulog, geokarag}@auth.gr). Their work has been supported by the THALES Project MIMOSA, co-financed by the European Union (European Social Fund-ESF) and Greek National Funds.

This work was presented in part at IEEE Globecom'13 Conference.

Digital Object Identifier 10.1109/TCOMM.2014.022314.130911

- We derive closed-form expressions for the outage probability of an OFDM dual-hop opportunistic AF relaying system, assuming that all nodes' analog RF front-ends are IQI-impaired. In addition, a general network topology is considered, where the relays (R) can be randomly positioned between the source (S) and the destination (D). Moreover, the direct link (DRL) between the S and D nodes is assumed to be in deep fade conditions.
- Next, we investigate the effect of the DRL between S and D on the system's performance, by deriving outage probability closed-form expressions for two different receiver types. More specifically, D performs either selection combining (SC) or maximum-ratio combining (MRC) on the received signals from the S node and the best relay.
- Towards a better understanding of the IQI effects on the outage probability, a special case, yet insightful, is considered where all the R nodes lie on the perpendicular line midway between S and D and with the same IQI level at all nodes. In this case, we derive functional dependence of the asymptotic outage probability floor on the signal constellation size, the number of relays, and IQI parameters.

Overall, the main result of this paper is that uncompensated IQI can be detrimental but it can also be effectively mitigated using a few relays. This result has a significant impact on relay deployment in future wireless communication networks.

B. Organization & Notations

The rest of the paper is organized as follows. The system model and the AF protocol are described in Section II. The outage probability is analyzed in Section III followed by simulation results in Section IV to validate our analysis. Finally, the paper is concluded in Section V.

Unless otherwise stated, lower and upper case bold letters denote vectors and matrices, respectively. The matrices $\mathbf{I}$ and $\mathbf{F}$ denote, respectively, the identity matrix and the Fast Fourier Transform (FFT) matrix whose middle row corresponds to the direct current (DC) and their subscripts denote their sizes. For matrices, $\mathbf{A}^{\sharp} \triangleq \tilde{\mathbf{I}}_N \mathbf{A}^* \tilde{\mathbf{I}}_N$, while for vectors, $\mathbf{a}^{\sharp} \triangleq \tilde{\mathbf{I}}_N \mathbf{a}^*$ is the reversal (image) permutation matrix. Also, $(\cdot)^H$, $(\cdot)^*$, $(\cdot)^T$ denote the matrix complex-conjugate transpose, complex-conjugate and transpose operations, respectively. The operators $\mathbb{E}[\cdot]$ and $|\cdot|$ denote the statistical expectation and the absolute value, respectively.

II. System Model

We consider the downlink transmission scenario in an AF OR system where each of the S, R and D nodes is equipped with a single antenna, as shown in Fig. 1. Furthermore, OFDM signalling is used in each of the two transmission time slots to combat the frequency selectivity of all the used channels, by dividing their wide frequency bandwidths into overlapping but orthogonal narrow-band subcarriers [21]. In the first slot, S transmits to the R and D nodes, while in the second slot, one relay is selected and used to amplify and forward the received signal to D, while the source and the other relays remain silent. The fading channels of all the links are assumed independent, frequency-selective and fixed over at least one OFDM symbol duration. The RF front-ends of the S, R and D nodes are assumed to be impaired with different IQI levels, as shown in Fig. 2. The R node suffers from both receive and transmit IQI. We consider frequency-independent IQI caused by the gain and the phase mismatches between the I and the Q branches denoted by $\epsilon_x^{t/r}$ and $\theta_x^{t/r}$, respectively, where x is the node identifier (S, R or D) and t/r denotes the up/down-conversion process, respectively. The time-domain (TD) baseband IQI-impaired signal is given by

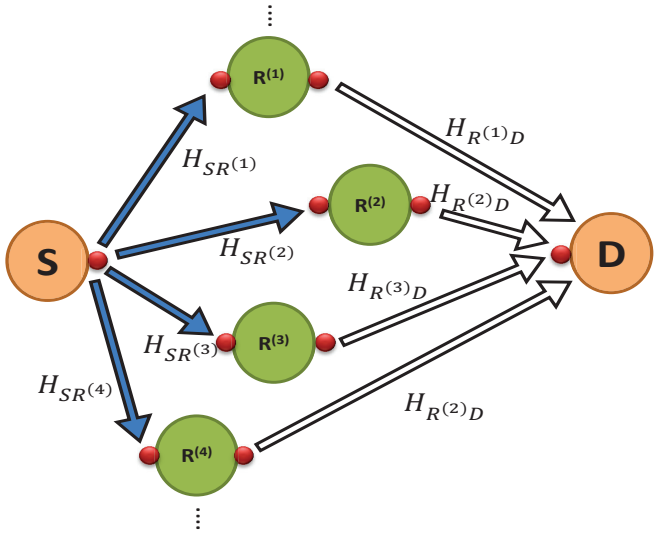

Fig. 1. System model block diagram where solid and hollow arrows show transmissions during the first and second time slots, respectively. The red bubbles indicate IQI, i.e. its presence on the RHS/LHS of the node means IQI at the Tx/Rx, respectively.

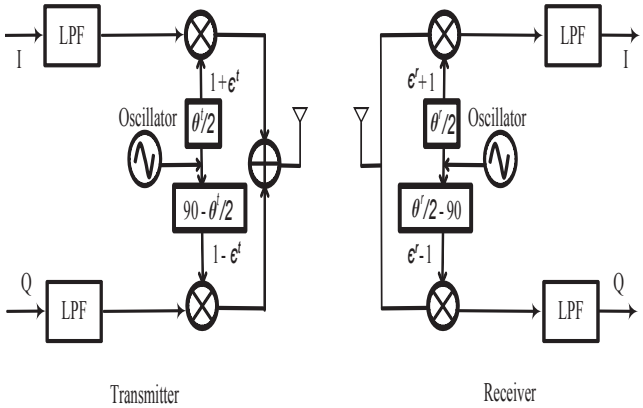

Fig. 2. IQI-impaired transceiver

$$g_{IQI}^{t/r}(t) = \mu_x^{t/r} g(t) + v_x^{t/r} g^*(t),$$

with

$$\mu_x^{t/r} = \cos\left(\frac{\theta_x^{t/r}}{2}\right) \mp j\epsilon_x^{t/r} \sin\left(\frac{\theta_x^{t/r}}{2}\right),$$

$$v_x^{t/r} = \epsilon_x^{t/r} \cos\left(\frac{\theta_x^{t/r}}{2}\right) - j \sin\left(\frac{\theta_x^{t/r}}{2}\right),$$

where the minus and plus signs denote the up and down-conversion processes, respectively. Note that $g(t)$ is the TD baseband IQI-free signal and the $g^*(t)$ term arises due to IQI [14]. Assuming that $\bar{\mathbf{s}}$ is the TD $N \times 1$ data vector with $\mathbb{E}\left[\bar{\mathbf{s}}\bar{\mathbf{s}}^H\right] = \eta_o \mathbf{I}_N$, the source transmits

$$\bar{\mathbf{s}}_S = \mu_S^t \bar{\mathbf{s}} + v_S^t \bar{\mathbf{s}}^*. \quad (1)$$

The TD received signals in the first time slot at the i^{th} R and D nodes after removing the cyclic-prefix (CP) are given,

respectively, by

$$\begin{aligned}\bar{\mathbf{r}}_R^{(i)} =&\mu_{R^{(i)}}^r \bar{\mathbf{H}}_{SR^{(i)}} \bar{\mathbf{s}}_S + v_{R^{(i)}}^r \left(\bar{\mathbf{H}}_{SR^{(i)}} \bar{\mathbf{s}}_S\right)^* + \\ &\mu_{R^{(i)}}^r \bar{\mathbf{n}}_{R^{(i)}} + v_{R^{(i)}}^r \bar{\mathbf{n}}_{R^{(i)}}^*, \\ \bar{\mathbf{r}}_D^{(1)} =&\mu_D^r \bar{\mathbf{H}}_{SD} \bar{\mathbf{s}}_S + v_D^r \left(\bar{\mathbf{H}}_{SD} \bar{\mathbf{s}}_S\right)^* + \mu_D^r \bar{\mathbf{n}}_D^{(1)} + v_D^r \bar{\mathbf{n}}_D^{(1)*},\end{aligned}$$

where $R^{(i)}$ denotes the i^{th} R node. The $N \times N$ circulant channel matrix $\bar{\mathbf{H}}_{IJ}$ models the channel impulse response (CIR) from node I to node J and its first column is $\left[\bar{h}_{IJ}^T 0_{1\times N-L}\right]^T$, with $\bar{h}_{IJ}$ is the CIR vector with L complex Gaussian taps. Moreover, $\bar{\mathbf{n}}_{R^{(i)}}$ and $\bar{\mathbf{n}}_D^{(1)}$ are the circularly symmetric complex additive white Gaussian noise (AWGN) vectors with single-sided power spectrum densities (PSD) of N_0.

From (1), $\bar{\mathbf{r}}_R^{(i)}$ and $\bar{\mathbf{r}}_D^{(1)}$ can be, respectively, written as

$$\begin{aligned}\bar{\mathbf{r}}_R^{(i)} =& \left(\mu_{R^{(i)}}^r \bar{\mathbf{H}}_{SR^{(i)}} \mu_S^t + v_{R^{(i)}}^r \bar{\mathbf{H}}_{SR^{(i)}}^* \left(v_S^t\right)^*\right) \bar{\mathbf{s}} \\ &+ \left(\mu_{R^{(i)}}^r \bar{\mathbf{H}}_{SR^{(i)}} v_S^t + v_{R^{(i)}}^r \bar{\mathbf{H}}_{SR^{(i)}}^* \left(\mu_S^t\right)^*\right) \bar{\mathbf{s}}^* \\ &+ \mu_{R^{(i)}}^r \bar{\mathbf{n}}_{R^{(i)}} + v_{R^{(i)}}^r \bar{\mathbf{n}}_{R^{(i)}}^*, \\ \bar{\mathbf{r}}_D^{(1)} =& \left(\mu_D^r \bar{\mathbf{H}}_{SD} \mu_S^t + v_D^r \bar{\mathbf{H}}_{SD}^* \left(v_S^t\right)^*\right) \bar{\mathbf{s}} \\ &+ \left(\mu_D^r \bar{\mathbf{H}}_{SD} v_S^t + v_D^r \bar{\mathbf{H}}_{SD}^* \left(\mu_S^t\right)^*\right) \bar{\mathbf{s}}^* \\ &+ \mu_D^r \bar{\mathbf{n}}_D^{(1)} + v_D^r \left(\bar{\mathbf{n}}_D^{(1)}\right)^*. \end{aligned} \quad (2)$$

According to the AF OR protocol, in the second time slot, the "best" relay (which we denote by R_*) amplifies the received signal and forwards it to the D node. To keep the relay complexity low, the channel is not estimated continuously at the relay. Hence, the amplification factor is defined as

$$\alpha \triangleq \sqrt{\frac{\eta_1}{\mathbb{E}\left[\left|\bar{\mathbf{r}}_{R_*}\right|^2\right]}},$$

where η_1 is the average transmitted signal energy at R_*. Therefore, the TD baseband equivalent signal transmitted by R_* in the second time slot is given by

$$\bar{\mathbf{s}}_{R_*} = \alpha \left\{\mu_{R_*}^t \bar{\mathbf{r}}_{R_*} + v_{R_*}^T \bar{\mathbf{r}}_{R_*}^*\right\}.$$

From (2), $\bar{\mathbf{s}}_{R_*}$ can be written as shown in (3), given at the top of this page. The best relay is selected following the rule

$$R_* = \arg\max_i \left(\gamma_{AF}^{(i)}(k)\right),$$

where $\gamma_{AF}^{(i)}(k)$ is the instantaneous SINR at the i^{th} relay [22]. The TD baseband equivalent signal received at the D node in the second time-slot is given by

$$\bar{\mathbf{r}}_D^{(2)} = \left(\mu_D^r \bar{\mathbf{H}}_1 + v_D^r \bar{\mathbf{H}}_2\right) \bar{\mathbf{s}} + \left(v_D^r \bar{\mathbf{H}}_1^* + \mu_D^r \bar{\mathbf{H}}_2^*\right) \bar{\mathbf{s}}^* + \bar{\mathbf{z}}, \quad (4)$$

where $\bar{\mathbf{H}}_1$, $\bar{\mathbf{H}}_2$, and $\bar{\mathbf{z}}$ are defined as follows

$$\begin{aligned}\bar{\mathbf{H}}_1 \triangleq& \alpha \bar{\mathbf{H}}_{R^{(i)}D} \\ &\left\{\mu_{R_*}^t \left[\mu_{R_*}^r \bar{\mathbf{H}}_{SR_*} \mu_S^t + v_{R_*}^r \bar{\mathbf{H}}_{SR_*}^* \left(v_S^t\right)^*\right]\right. \\ &\left. + v_{R_*}^t \left[\left(\mu_{R_*}^r\right)^* \bar{\mathbf{H}}_{SR_*}^* \left(v_S^t\right)^* + \left(v_{R_*}^r\right)^* \bar{\mathbf{H}}_{SR_*} \mu_S^t\right]\right\}, \end{aligned} \quad (5)$$

$$\begin{aligned}\bar{\mathbf{H}}_2 \triangleq& \alpha \bar{\mathbf{H}}_{R_*D}^* \\ &\left\{\left(\mu_{R_*}^t\right)^* \left[\left(\mu_{R_*}^r\right)^* \bar{\mathbf{H}}_{SR_*}^* \left(v_S^t\right)^* + \left(v_{R_*}^r\right)^* \bar{\mathbf{H}}_{SR_*} \left(\mu_S^t\right)\right]\right. \\ &\left. + \left(v_{R_*}^t\right)^* \left[\mu_{R_*}^r \bar{\mathbf{H}}_{SR_*} \mu_S^t + v_{R_*}^r \bar{\mathbf{H}}_{SR_*}^* \left(v_S^t\right)^*\right]\right\}, \end{aligned} \quad (6)$$

$$\begin{aligned}\bar{\mathbf{z}} \triangleq& \mu_D^r \bar{\mathbf{H}}_{R_*D} \alpha \left\{\mu_{R_*}^t \left[\mu_{R_*}^r \bar{\mathbf{n}}_{R_*} + v_{R_*}^r \bar{\mathbf{n}}_{R_*}^*\right]\right. \\ &\left. + v_{R_*}^t \left[\left(\mu_{R_*}^r\right)^* \bar{\mathbf{n}}_{R_*}^* + \left(v_{R_*}^r\right)^* \bar{\mathbf{n}}_{R_*}\right]\right\} \\ &+ v_{R_*}^r \bar{\mathbf{H}}_{R_*D}^* \alpha \left\{\left(\mu_{R_*}^t\right)^* \left[\left(\mu_{R_*}^r\right)^* \bar{\mathbf{n}}_{R_*}^* + \left(v_{R_*}^r\right)^* \bar{\mathbf{n}}_{R_*}\right]\right. \\ &\left. + \left(v_{R_*}^t\right)^* \left[\mu_{R_*}^r \bar{\mathbf{n}}_{R_*} + v_{R_*}^r \bar{\mathbf{n}}_{R_*}^*\right]\right\} \\ &+ \mu_D^r \bar{\mathbf{n}}_D + v_D^r \bar{\mathbf{n}}_D^*. \end{aligned}$$

Therefore, the frequency-domain (FD) received signal at the D node in the second time slot is obtained by taking the FFT of (4), and can be written as follows

$$\mathbf{r}_D^{(2)} = \left(\mu_D^r \mathbf{H}_1 + v_D^r \mathbf{H}_2\right) \mathbf{s} + \left(v_D^r \mathbf{H}_1^\sharp + \mu_D^r \mathbf{H}_2^\sharp\right) \mathbf{s}^\sharp + \mathbf{z}. \quad (7)$$

In (7), $\mathbf{H}_1$ and $\mathbf{H}_2$ can be easily obtained from (5) and (6) by replacing each $\bar{\mathbf{H}}_{IJ}$ and $\bar{\mathbf{H}}_{IJ}^*$ by $\mathbf{H}_{IJ}$ and $\mathbf{H}_{IJ}^\sharp$, respectively, where $\mathbf{H}_{IJ}$ is the $N \times N$ diagonal matrix whose diagonal elements are the channel frequency response (CFR) coefficients from node I to node J and $\mathbf{H}_{IJ}(k)$ is the k^{th} element on the main diagonal of $\mathbf{H}_{IJ}$. In addition, the vectors $\mathbf{s}$ and $\mathbf{z}$ are the frequency-domain representations of $\bar{\mathbf{s}}$ and $\bar{\mathbf{z}}$, respectively. It is evident from (7) that IQI results in image (mirror) interference in FD where the k^{th} subcarrier is distorted by its image subcarrier whose index is denoted by $(-k)$.

III. Performance Analysis

In this section, we investigate the effect of IQI on the system's outage performance, if perfect global channel state information (CSI) knowledge is assumed[1]. First, we derive the instantaneous SINR expressions in Section III-A for the $S \to D$, $S \to R^{(i)}$ and $R^{(i)} \to D$ links and then we use these expressions to evaluate the end-to-end outage probability, which is defined as the probability that the SINR falls below a given threshold. In Section III-B1, we analyze the outage probability when the DRL between the nodes S and D is in deep shadow-fading conditions. On the other hand, when communication between the S and D nodes occurs through the direct and indirect (via relaying) links, the outage is investigated assuming both SC and MRC combining in Sections III-B2 and III-B3, respectively. We conclude with remarks on extending the outage probability analysis to decode-and-forward relaying (DF) in Section III-C.

A. Instantaneous SINR

*1) **Direct link**:* From (2), the SINR at the k^{th} subcarrier in the direct mode is given by

$$\gamma_{SD}(k) = \frac{\left|\widetilde{Z}_{SD}\right|^2}{\left|\widetilde{W}_{SD}\right|^2 + N_{SD}} \triangleq \frac{Z_{SD}}{W_{SD} + N_{SD}}, \quad (8)$$

[1]The case of imperfect CSI due to IQI and outdated estimation will not be investigated due to space limitations. However, the performance results presented here are upper bounds to those when imperfect CSI is assumed.

$$\begin{aligned}\bar{\mathbf{s}}_{R_*} &= \alpha\left\{\mu^t_{R_*}\left[\mu^r_{R_*}\bar{\mathbf{H}}_{SR_*}\mu^t_S + v^r_{R_*}\bar{\mathbf{H}}^*_{SR_*}\left(v^t_s\right)^*\right] + v^t_{R_*}\left[\left(\mu^r_{R_*}\right)^*\bar{\mathbf{H}}^*_{SR_*}\left(v^t_S\right)^* + \mu^t_s\bar{\mathbf{H}}_{SR_*}\left(v^r_{R_*}\right)^*\right]\right\}\bar{\mathbf{s}}\\ &+ \alpha\left\{\mu^t_{R_*}\left[\mu^r_{R_*}\bar{\mathbf{H}}_{SR_*}v^t_S + v^r_{R_*}\bar{\mathbf{H}}^*_{SR_*}\left(\mu^t_S\right)^*\right] + v^t_{R_*}\left[\left(\mu^r_{R_*}\right)^*\bar{\mathbf{H}}^*_{SR_*}\left(\mu^t_S\right)^* + \left(v^r_{R_*}\right)^*\bar{\mathbf{H}}_{SR_*}v^t_S\right]\right\}\bar{\mathbf{s}}^*\\ &+ \alpha\mu^t_{R_*}\left[\mu^r_{R_*}\bar{\mathbf{n}}_{R_*} + v^r_{R_*}\bar{\mathbf{n}}^*_{R_*}\right] + \alpha v^t_{R_*}\left[\left(\mu^r_{R_*}\right)^*\bar{\mathbf{n}}^*_{R_*} + \left(v^r_{R_*}\right)^*\bar{\mathbf{n}}_{R_*}\right]\end{aligned} \tag{3}$$

where

$$\begin{aligned}\widetilde{Z}_{SD} &\triangleq a_{SD}\mathbf{H}_{SD}(k) + b_{SD}\mathbf{H}^*_{SD}(-k),\\ \widetilde{W}_{SD} &\triangleq c_{SD}\mathbf{H}_{SD}(k) + d_{SD}\mathbf{H}^*_{SD}(-k),\\ N_{SD} &\triangleq \frac{N_0}{\eta_o}\left(|\mu^r_D|^2 + |v^r_D|^2\right),\end{aligned}$$

with $a_{SD} \triangleq \mu^r_D\mu^t_S$, $b_{SD} \triangleq v^r_D\left(v^t_S\right)^*$, $c_{SD} \triangleq \mu^r_D v^t_S$ and $d_{SD} \triangleq v^r_D\left(\mu^t_S\right)^*$.

To simplify $\gamma_{SD}(k)$ in (8), we use the fact that for practical IQI levels, amplitude and phase imbalances less than 1 dB and 5°, respectively, $b_{SD} \simeq 0$. Moreover, except for few central subcarriers, the correlation between the k^{th} subcarrier and its image is small due to their large spectral separation, hence, they can be assumed independent. Therefore

$$2\mathbb{E}\left[\Re\left\{c_{SD}d^*_{SD}\mathbf{H}^*_{SD}(k)\,\mathbf{H}^*_{SD}(-k)\right\}\right] \simeq 0.$$

Consequently, we can approximate Z_{SD} and W_{SD} as follows

$$\begin{aligned}Z_{SD} &\simeq |a_{SD}|^2\,|\mathbf{H}_{\text{SD}}(k)|^2,\\ W_{SD} &= |c_{SD}\mathbf{H}_{\text{SD}}(k) + d_{SD}\mathbf{H}^*_{\text{SD}}(-k)|^2\\ &\simeq |c_{SD}\mathbf{H}_{\text{SD}}(k)|^2 + |d_{SD}\mathbf{H}^*_{\text{SD}}(-k)|^2,\end{aligned}$$

where $|\mathbf{H}_{IJ}(k)|^2$ is an exponential random variable[2] (RV) with mean λ^k_{IJ} proportional to $(d_{IJ})^{-\xi}$ where d_{IJ} is the distance between nodes I and J with path loss exponent ξ.

*2) **AF OR protocol**:* The selected relay is assumed to be the one with the highest instantaneous SINR $\gamma^{(i)}_{AF}(k)$, which can be determined as follows

$$\gamma_{AF}(k) = \max_{i\in\{1,\ldots,N\}}\gamma^{(i)}_{AF}(k),$$

where $\gamma^{(i)}_{AF}(k)$ is given by [13],

$$\begin{aligned}\gamma^{(i)}_{AF}(k) &= \frac{\gamma^{(i)}_{SR}(k)\,\gamma^{(i)}_{RD}(k)}{\gamma^{(i)}_{SR}(k) + \gamma^{(i)}_{RD}(k) + 1} \le \frac{\gamma^{(i)}_{SR}(k)\,\gamma^{(i)}_{RD}(k)}{\gamma^{(i)}_{SR}(k) + \gamma^{(i)}_{RD}(k)}\\ &\le \min\left(\gamma^{(i)}_{SR}(k), \gamma^{(i)}_{RD}(k)\right).\end{aligned} \tag{9}$$

In the sequel, we consider that $\gamma^{(i)}_{AF}(k)$ is given by $\min\left(\gamma^{(i)}_{SR}(k), \gamma^{(i)}_{RD}(k)\right)$ which is an upper bound and accurate approximation for the instantaneous SINR of AF-relaying, where $\gamma^{(i)}_{SR}(k)$ and $\gamma^{(i)}_{RD}(k)$ denote the instantaneous SINR between $S \rightarrow R^{(i)}$ and $R^{(i)} \rightarrow D$ links, respectively, and they can be evaluated from Eqns. (10) and (11), on the top of the next page. Note that the upper bound in (9) is also a very good approximation especially in the high SNR regime, as stated in [24]. Similar to $\gamma_{SD}(k)$, both $\gamma^{(i)}_{SR}(k)$ and $\gamma^{(i)}_{RD}(k)$ can be approximated as

$$\gamma_{SR^{(i)}}(k) \simeq \frac{\left|\widetilde{Z}_{SR^{(i)}}\right|^2}{\left|\widetilde{W}_{SR^{(i)}}\right|^2 + N_{SR^{(i)}}} \triangleq \frac{Z_{SR^{(i)}}}{W_{SR^{(i)}} + N_{SR^{(i)}}},$$

$$\gamma_{R^{(i)}D}(k) \simeq \frac{\left|\widetilde{Z}_{R^{(i)}D}\right|^2}{\left|\widetilde{W}_{R^{(i)}D}\right|^2 + N_{R^{(i)}D}} \triangleq \frac{Z_{R^{(i)}D}}{W_{SR^{(i)}} + N_{R^{(i)}D}},$$

where

$$\begin{aligned}Z_{SR^{(i)}} &\triangleq \left|a^{(i)}_{SR^{(i)}}\right|^2|\mathbf{H}_{SR^{(i)}}(k)|^2,\\ W_{SR^{(i)}} &\triangleq \left|c^{(i)}_{SR^{(i)}}\mathbf{H}_{SR^{(i)}}(k)\right|^2 + \left|d^{(i)}_{SR^{(i)}}\mathbf{H}^*_{SR^{(i)}}(-k)\right|^2,\\ N_{SR^{(i)}} &\triangleq \frac{N_o}{\eta_o}\left(|\mu^r_{R^{(i)}}|^2 + |v^r_{R^{(i)}}|^2\right),\end{aligned}$$

with $a^{(i)}_{SR^{(i)}} \triangleq \mu^r_{R^{(i)}}\mu^t_S$, $c^{(i)}_{SR^{(i)}} \triangleq \mu^r_{R^{(i)}}v^t_S$, $d^{(i)}_{SR^{(i)}} \triangleq v^r_{R^{(i)}}\left(\mu^t_S\right)^*$, and

$$\begin{aligned}Z_{R^{(i)}D} &\triangleq \left|a^{(i)}_{R^{(i)}D}\right|^2|\mathbf{H}_{R^{(i)}D}(k)|^2,\\ W_{R^{(i)}D} &\triangleq \left|c^{(i)}_{R^{(i)}D}\mathbf{H}_{R^{(i)}D}(k)\right|^2 + \left|d^{(i)}_{R^{(i)}D}\mathbf{H}^*_{R^{(i)}D}(-k)\right|^2,\\ N_{R^{(i)}D} &\triangleq \frac{N_o}{\eta_1}\left(|\mu^r_D|^2 + |v^r_D|^2\right),\end{aligned}$$

with $a^{(i)}_{R^{(i)}D} \triangleq \mu^r_D\mu^t_{R^{(i)}}$, $c^{(i)}_{R^{(i)}D} \triangleq \mu^r_D v^t_{R^{(i)}}$, $d^{(i)}_{R^{(i)}D} \triangleq v^r_D\left(\mu^t_{R^{(i)}}\right)^*$.

B. Outage Probability Analysis

*1) **Without Direct Link**:* The end-to-end outage probability (outage rate), when the DRL is assumed weak enough to be ignored, is given by [25]

$$\begin{aligned}P_{AF} &= P_r\left(\log_2(1+\gamma_{AF}(k)) \le r_{\text{th}}\right)\\ &= P_r\left(\gamma_{AF}(k) \le \gamma_{\text{th}}\right) = \prod_{i=1}^{N_r}P_{AF^{(i)}}\left(\gamma^{(i)}_{AF}(k) \le \gamma_{\text{th}}\right),\end{aligned} \tag{12}$$

where r_{th} is the minimum allowable (threshold) rate[3], $\gamma_{\text{th}} = 2^{r_{\text{th}}} - 1$, and $P_{AF^{(i)}}\left(\gamma^{(i)}_{AF}(k) \le u\right)$ is the cumulative density function (CDF) of $\gamma^{(i)}_{AF}(k)$ which can be approximated as

$$\begin{aligned}P_{AF^{(i)}}&\left(\gamma^{(i)}_{AF}(k) \le 2^{r_{\text{th}}} - 1\right) \simeq\\ &1 - \left[1 - F_{\gamma^{(i)}_{SR}}(\gamma_{\text{th}})\right]\left[1 - F_{\gamma^{(i)}_{RD}}(\gamma_{\text{th}})\right],\end{aligned} \tag{13}$$

[2]The CFR is a linear transformation of L-tap cpmplex Gaussian CIR [23]. Hence, it is also a Gaussian RV and its magnitude square is an exponential RV.

[3]Because the communication occurs over two time slots, r_{th} is half the transmission rate.

$$\gamma_{SR}^{(i)}(k)=\frac{\left|\mu_{R^{(i)}}^{r}\mu_{S}^{t}\mathbf{H}_{SR^{(i)}}(k)+v_{R^{(i)}}^{r}\left(v_{S}^{t}\right)^{*}\mathbf{H}_{SR^{(i)}}^{*}(-k)\right|^{2}}{\left|\mu_{R^{(i)}}^{r}v_{S}^{t}\mathbf{H}_{SR^{(i)}}(k)+v_{R^{(i)}}^{r}\left(\mu_{S}^{t}\right)^{*}\mathbf{H}_{SR^{(i)}}^{*}(-k)\right|^{2}+\frac{N_0}{\eta_o}\left(\left|\mu_{R^{(i)}}^{r}\right|^{2}+\left|v_{R^{(i)}}^{r}\right|^{2}\right)} \tag{10}$$

$$\gamma_{RD}^{(i)}(k)=\frac{\left|\mu_{D}^{r}\mu_{R^{(i)}}^{t}\mathbf{H}_{R^{(i)}D}(k)+v_{D}^{r}\left(v_{R^{(i)}}^{t}\right)^{*}\mathbf{H}_{R^{(i)}D}^{*}(-k)\right|^{2}}{\left|\mu_{D}^{r}v_{R^{(i)}}^{t}\mathbf{H}_{R^{(i)}D}(k)+v_{D}^{r}\left(\mu_{R^{(i)}}^{t}\right)^{*}\mathbf{H}_{R^{(i)}D}^{*}(-k)\right|^{2}+\frac{N_0\left(\left|\mu_{D}^{r}\right|^{2}+\left|v_{D}^{r}\right|^{2}\right)}{\eta_1\left|\mu_{R^{(i)}}^{r}\right|^{2}}} \tag{11}$$

where $F_{\gamma_{SR}^{(i)}}(\gamma_{\text{th}})$ and $F_{\gamma_{RD}^{(i)}}(\gamma_{\text{th}})$ are the CDFs of $\gamma_{SR}^{(i)}(k)$ and $\gamma_{RD}^{(i)}(k)$, respectively. To evaluate the CDF of $\gamma_{SR}^{(i)}$, we re-write (10) as follows

$$\gamma_{SR}^{(i)}(k)\simeq\frac{\left|a_{SR^{(i)}}^{(i)}\right|^{2}\left|H_{SR^{(i)}}(k)\right|^{2}}{\left|c_{SR^{(i)}}^{(i)}H_{SR^{(i)}}(k)\right|^{2}+\left|d_{SR^{(i)}}^{(i)}H_{SR^{(i)}}^{*}(-k)\right|^{2}+N_{SR^{(i)}}}\triangleq\frac{a_{SR}^{(i)}X}{c_{SR}^{(i)}X+d_{SR}^{(i)}Y+N_{SR^{(i)}}}, \tag{14}$$

with $a_{SR}^{(i)}\triangleq\left|a_{SR^{(i)}}^{(i)}\right|^{2}$, $c_{SR}^{(i)}\triangleq\left|c_{SR^{(i)}}^{(i)}\right|^{2}$, $d_{SR}^{(i)}\triangleq\left|d_{SR^{(i)}}^{(i)}\right|^{2}$, and X and Y are exponentially-distributed RVs with mean $\lambda_{SR^{(i)}}^{k}$ and $\lambda_{SR^{(i)}}^{-k}$, respectively. Moreover, exploiting the independence between X and Y, we evaluate the CDF of $\gamma_{SR}^{(i)}(k)$ as follows [25]

$$F_{\gamma_{SR}^{(i)}}(\gamma_{\text{th}})=\begin{cases}\int_{0}^{\infty}P_X\left(x\le\frac{\gamma_{\text{th}}\left(d_{SR}^{(i)}y+N_{SR^{(i)}}\right)}{a_{SR}^{(i)}-\gamma_{\text{th}}c_{SR}^{(i)}}\right)P_Y(y)\,dy, & \gamma_{\text{th}}\le\frac{a_{SR}^{(i)}}{c_{SR}^{(i)}}\\ 1, & \text{otherwise}\end{cases} \tag{15}$$

Carrying out the integration in (15), we get

$$F_{\gamma_{SR}^{(i)}}(\gamma_{\text{th}})=1-\frac{\lambda_{SR^{(i)}}^{k}\left(a_{SR}^{(i)}-\gamma_{\text{th}}c_{SR}^{(i)}\right)}{\lambda_{SR^{(i)}}^{k}\left(a_{SR}^{(i)}-\gamma_{\text{th}}c_{SR}^{(i)}\right)+d_{SR}^{(i)}\gamma_{\text{th}}\lambda_{SR^{(i)}}^{-k}}\times e^{-\frac{N_{SR^{(i)}}\gamma_{\text{th}}}{\left(-a_{SR}^{(i)}+\gamma_{\text{th}}c_{SR}^{(i)}\right)\lambda_{SR^{(i)}}^{k}}},\qquad \gamma_{\text{th}}\le\frac{a_{SR}^{(i)}}{c_{SR}^{(i)}} \tag{16}$$

Hereafter, the condition on γ_{th} is omitted for notational convenience since it is obvious that the outage probability becomes equal to one if this condition is not satisfied. Moreover, assuming uncorrelated scattering, $\lambda_{SR^{(i)}}^{k}=\lambda_{SR^{(i)}}^{-k}=\lambda_{SR^{(i)}}$, and Eqn. (16) can be further simplified as

$$F_{\gamma_{SR}^{(i)}}(\gamma_{\text{th}})=1-\frac{\left(a_{SR}^{(i)}-\gamma_{\text{th}}c_{SR}^{(i)}\right)}{\left(a_{SR}^{(i)}-\gamma_{\text{th}}c_{SR}^{(i)}\right)+d_{SR}^{(i)}\gamma_{\text{th}}}e^{-\frac{N_{SR^{(i)}}\gamma_{\text{th}}}{\left(-a_{SR}^{(i)}+\gamma_{\text{th}}c_{SR}^{(i)}\right)\lambda_{SR^{(i)}}}}. \tag{17}$$

Similarly,

$$F_{\gamma_{RD}^{(i)}}(\gamma_{\text{th}})=1-\frac{\left(a_{RD}^{(i)}-\gamma_{\text{th}}c_{RD}^{(i)}\right)}{\left(a_{RD}^{(i)}-\gamma_{\text{th}}c_{RD}^{(i)}\right)+d_{RD}^{(i)}\gamma_{\text{th}}}e^{-\frac{N_{R^{(i)}D}\gamma_{\text{th}}}{\left(-a_{RD}^{(i)}+\gamma_{\text{th}}c_{RD}^{(i)}\right)\lambda_{R^{(i)}D}}}, \tag{18}$$

where $a_{RD}^{(i)}\triangleq\left|a_{R^{(i)}D}^{(i)}\right|^{2}=\left|\mu_{D}^{r}\mu_{R^{(i)}}^{t}\right|^{2}$, $c_{RD}^{(i)}\triangleq\left|c_{R^{(i)}D}^{(i)}\right|^{2}=\left|\mu_{D}^{r}v_{R^{(i)}}^{t}\right|^{2}$, $d_{RD}^{(i)}\triangleq\left|d_{R^{(i)}D}^{(i)}\right|^{2}=\left|v_{D}^{r}\left(\mu_{R^{(i)}}^{t}\right)^{*}\right|^{2}$ and $N_{R^{(i)}D}\triangleq\frac{N_0\left(|\mu_{D}^{r}|^{2}+|v_{D}^{r}|^{2}\right)}{\eta_1\left|\mu_{R^{(i)}}^{r}\right|^{2}}$.

Substituting from Eqns. (17) and (18) into (13) to derive $P_{AF^{(i)}}\ \forall i$ and then substituting the result into (12), we get

$$P_{AF}(\gamma_{\text{th}})\simeq\prod_{i\in\mathcal{W}}\left(1-\frac{\left(a_{SR}^{(i)}-\gamma_{\text{th}}c_{SR}^{(i)}\right)\left(a_{RD}^{(i)}-\gamma_{\text{th}}c_{RD}^{(i)}\right)}{\left[\left(a_{SR}^{(i)}-\gamma_{\text{th}}c_{SR}^{(i)}\right)+d_{SR}^{(i)}\gamma_{\text{th}}\right]\left[\left(a_{RD}^{(i)}-\gamma_{\text{th}}c_{RD}^{(i)}\right)+d_{RD}^{(i)}\gamma_{\text{th}}\right]}\times e^{-\frac{N_{SR^{(i)}}\gamma_{\text{th}}}{\left(-a_{SR}^{(i)}+\gamma_{\text{th}}c_{SR}^{(i)}\right)\lambda_{SR^{(i)}}}-\frac{N_{R^{(i)}D}\gamma_{\text{th}}}{\left(-a_{RD}^{(i)}+\gamma_{\text{th}}c_{RD}^{(i)}\right)\lambda_{R^{(i)}D}}}\right). \tag{19}$$

where $\mathcal{W}=\left\{i:i\in\{1,\ldots,N_r\}\ \&\gamma_{th}\le\min\left\{\frac{a_{SR}^{(i)}}{c_{SR}^{(i)}},\frac{a_{RD}^{(i)}}{c_{RD}^{(i)}}\right\}\right\}$.

An Insightful Special Case

To gain more insight, we investigate a special case, where all nodes suffer from the same IQI level and the relay nodes lie on the perpendicular line midway between the S and D nodes. In this case, Eqn. (19) reduces to

$$P_{AF}=\prod_{i=1}^{N_r}\left(1-\left(\frac{1}{1+\eta}\right)^{2}e^{-\frac{\left(N_{SR^{(i)}}+N_{R^{(i)}D}\right)\gamma_{\text{th}}}{\left(-a+\gamma_{\text{th}}c\right)\lambda^{(i)}}}\right), \tag{20}$$

where $\eta\triangleq\frac{c\gamma_{\text{th}}}{-c\gamma_{\text{th}}+a}$, $a\triangleq|\mu|^{4}$, $c\triangleq|\mu v|^{2}$, and $\lambda^{(i)}\triangleq\lambda_{SR^{(i)}}=\lambda_{R^{(i)}D}$ for the i^{th} relay node. Moreover, in the high-SNR regime ($N_{SR^{(i)}}$, $N_{R^{(i)D}}\to 0$) the outage probability floor is given by

$$P_{AF}\doteq\left(1-\left(\frac{1}{1+\eta}\right)^{2}\right)^{N_r}, \tag{21}$$

where $\doteq$ denotes the asymptotic equivalence at high SNR. Furthermore, for practical IQI levels and transmission rates, $\eta\simeq\frac{c\gamma_{\text{th}}}{a}<<1$. Therefore, (21) can be approximated as

$$P_{AF}\doteq\left(1-(1+\eta)^{-2}\right)^{N_r}\simeq(1-(1-2\eta))^{N_r}\simeq 2^{N_r}\eta^{N_r}\simeq 2^{N_r}\frac{c^{N_r}\gamma_{\text{th}}^{N_r}}{a^{N_r}}\simeq\left(2\left|\frac{\nu}{\mu}\right|^{2}\left(2^{r_{\text{th}}}-1\right)\right)^{N_r}, \tag{22}$$

where $\left|\frac{\nu}{\mu}\right|^{2}$ represents the IQI interference-to-signal ratio which is typically $<<1$. From Eqn. (22), it is evident that the outage probability floor decreases exponentially at a rate of N_r for a given signal constellation size. Hence, the diversity effect of OR reduces the IQI outage floor significantly, even for few relays. On the other hand, the outage probability floor worsens as the signal constellation size increases due

to the increased sensitivity of bigger signal constellation to IQI effects. Furthermore, Eqn. (22) shows that the outage probability floor is independent of the relays' positions on the perpendicular line midway between S and D.

*2) **With Direct Link and SC at the Destination**:* Next, we analyze the outage probability when the DRL is sufficiently strong not to be ignored. In this case, it is assumed that the D node performs SC on the received signals in the first and second time slots assuming perfect CSI knowledge. Therefore, the SINR at the k^{th} subcarrier is given by [26]

$$\gamma_{SRD}^{(SC)}(k) = \max\left(\gamma_{SD}(k), \gamma_{AF}(k)\right).$$

Hence, the outage probability can be written as follows [27]

$$\begin{aligned} P_{SRD}^{(SC)} &= P_r\left(\gamma_{SRD}^{(SC)} \le \gamma_{th}\right) \\ &= P_r\left(\gamma_{SD}(k) \le \gamma_{th}\right) P_r\left(\gamma_{AF}(k) \le \gamma_{th}\right), \end{aligned} \quad (23)$$

where $P_r\left(\gamma_{SD}(k) \le \gamma_{th}\right)$ is the CDF of γ_{SD}, which can be evaluated similar to (17) as

$$F_{\gamma_{SD}}(\gamma_{\text{th}}) = 1 - \frac{(a_{SD} - \gamma_{\text{th}} c_{SD})}{(a_{SD} - \gamma_{\text{th}} c_{SD}) + d_{SD}\gamma_{\text{th}}} e^{-\frac{N_{SD}\gamma_{\text{th}}}{(-a_{SD}+\gamma_{\text{th}}c_{SD})\lambda_{SD}}}, \quad (24)$$

and $P_r\left(\gamma_{AF}(k) \le \gamma_{th}\right)$ is given by (19). Substituting Eqns. (24) and (19) into (23), we get

$$\begin{aligned} P_{SRD}^{(SC)}(\gamma_{\text{th}}) = &\left(1 - \frac{(a_{SD} - \gamma_{\text{th}} c_{SD})}{(a_{SD} - \gamma_{\text{th}} c_{SD}) + d_{SD}\gamma_{\text{th}}} e^{-\frac{N_{SD}\gamma_{\text{th}}}{(-a_{SD}+\gamma_{\text{th}}c_{SD})\lambda_{SD}}}\right) \prod_{i=1}^{N_r} \Bigg(1 \\ &- \frac{\left(a_{SR}^{(i)} - \gamma_{\text{th}} c_{SR}^{(i)}\right)\left(a_{RD}^{(i)} - \gamma_{\text{th}} c_{RD}^{(i)}\right)}{\left[\left(a_{SR}^{(i)} - \gamma_{\text{th}} c_{SR}^{(i)}\right) + d_{SR}^{(i)}\gamma_{\text{th}}\right]\left[\left(a_{RD}^{(i)} - \gamma_{\text{th}} c_{RD}^{(i)}\right) + d_{RD}^{(i)}\gamma_{\text{th}}\right]} \\ &\times e^{-\frac{N_{SR^{(i)}}\gamma_{\text{th}}}{\left(-a_{SR}^{(i)}+\gamma_{\text{th}}c_{SR}^{(i)}\right)\lambda_{SR^{(i)}}} - \frac{N_{R^{(i)}D}\gamma_{\text{th}}}{\left(-\alpha_{RD}^{(i)}+\gamma_{\text{th}}c_{RD}^{(i)}\right)\lambda_{R^{(i)}D}}}\Bigg). \end{aligned} \quad (25)$$

Considering the special case of interest where all nodes suffer from the same IQI level, (25) simplifies to the following expression

$$\begin{aligned} P_{SRD}^{(SC)} = &\left(1 - \left(\frac{1}{1+\eta}\right)^2 e^{-\frac{N_{SD}\gamma_{th}}{(-a_{SD}+\gamma_{th}c_{SD})\lambda_{SD}}}\right) \\ &\prod_{i=1}^{N_r}\left(1 - \left(\frac{1}{1+\eta}\right)^2 e^{-\frac{\left(N_{SR^{(i)}}+N_{R^{(i)}D}\right)\gamma_{\text{th}}}{(-a+\gamma_{\text{th}}c)\lambda^{(i)}}}\right). \end{aligned} \quad (26)$$

In the high-SNR regime ($N_{SD}, N_{SR^{(i)}}, N_{R^{(i)}D} \to 0$), the outage probability floor is given by

$$P_{SRD}^{(SC)} \doteq \left(1 - \left(\frac{1}{1+\eta}\right)^2\right)^{N_r+1}. \quad (27)$$

For practical IQI levels, Eqn. (27) can be approximated as

$$P_{SRD}^{(SC)} \doteq \left(1 - (1-\eta)^2\right)^{N_r+1} \simeq \left(2\left|\frac{v}{\mu}\right|^2 (2^{r_{th}} - 1)\right)^{N_r+1}. \quad (28)$$

From Eqn. (28), it is evident that for AF OR with DRL and SC at the D node, the outage probability floor decreases exponentially at rate of $(N_r + 1)$ for a given signal constellation size, while in AF OR without DRL scenarios, the exponential decrease is at rate of N_r only for the same constellation size. Hence, the presence of the DRL and the use of SC provide higher tolerance to IQI effects compared to AF OR without DRL. Moreover, the diversity effect of AF OR with the DRL reduces the IQI outage floor even further in comparison with the case of no DRL, since the DRL acts like an extra degree of diversity.

*3) **With Direct Link and MRC at the Destination**:* In this case, the D node performs maximum-ratio combining (MRC) on the received signals in the first and second time slots assuming perfect CSI knowledge [28]. Therefore, the SINR at the k^{th} subcarrier can be bounded [13] as follows

$$\gamma_{SRD}^{(MRC)}(k) \le \gamma_{SD}(k) + \gamma_{AF}(k), \quad (29)$$

where $\gamma_{SD}(k)$ is the instantaneous SINR at subcarrier k of the $S \to D$ link and it can be evaluated similar to (10) by replacing $\mu_{R^{(i)}}^r$, $\nu_{R^{(i)}}^r$, and $\mathbf{H}_{SR^{(i)}}$ with μ_D^r, ν_D^r, and $\mathbf{H}_{SD}$, respectively. Hence, the outage probability is given by

$$\begin{aligned} P_{SRD}^{(MRC)} &= P_r\left(\gamma_{SRD}^{(MRC)} \le \gamma_{\text{th}}\right) \\ &\simeq \int_0^{\gamma_{\text{th}}} P_{AF}(\gamma_{\text{th}} - u) f_{SD}(u) du, \end{aligned} \quad (30)$$

where $f_{SD}(u)$ is the PDF of γ_{SD}, $f_{SD}(u) = \frac{\partial F_{SD}(u)}{\partial u}$, and $F_{SD}(u)$ can be obtained in a manner similar to (17) by replacing the relay's parameters with those of the D node.

To obtain a tractable expression for the outage probability, we consider the high-SNR regime which is of particular interest since the performance is interference limited, due to IQI, rather than noise limited. Therefore, as $N_{SR^{(i)}} \to 0$, $N_{R^{(i)}D} \to 0 \ \forall\ i \in \{1, \cdots, N_r\}$, and $N_{SD} \to 0$, the asymptotic outage probability is given by

$$P_{SRD}^{(MRC)} \doteq \int_0^{\gamma_{th}} \lim_{N_{SR^{(i)}}, N_{R^{(i)}D} \to 0} P_{AF}(\gamma_{\text{th}} - u) \lim_{N_{SD}\to 0} f_{SD}(u) du, \quad \forall\ i \in \{1, \cdots, N_r\}, \quad (31)$$

where $\lim_{N_{SD}\to 0} f_{SD}(\gamma_{\text{th}})$ can be approximated as

$$\begin{aligned} \lim_{N_{SD}\to 0} f_{SD}(\gamma_{\text{th}}) &= \frac{d_{SD}}{a_{SD}} \frac{1}{\left(1 + \tau_{SD}\gamma_{\text{th}}\right)^2} \\ &\simeq \frac{d_{SD}}{a_{SD}} \left(1 - 2\ \tau_{SD}\ \gamma_{\text{th}}\right), \end{aligned} \quad (32)$$

where $a_{SD} \triangleq \left|\mu_D^r \mu_S^t\right|^2$, $c_{SD} \triangleq \left|\mu_D^r v_S^t\right|^2$, $d_{SD} \triangleq \left|v_D^r \left(\mu_S^t\right)^*\right|^2$, and $\tau_{SD} \triangleq \frac{d_{SD} - c_{SD}}{a_{SD}}$. Since d_{SD} and c_{SD} are in the same order of magnitude and $\frac{c_{SD}}{a_{SD}}\gamma_{\text{th}} << 1$, it can be easily shown that the quantity $\tau_{SD}\ \gamma_{\text{th}} << 1$. Hence, $\left(1 + \tau_{SD}\gamma_{\text{th}}\right)^{-2} \simeq$

$(1-2\tau_{SD}\gamma_{\text{th}})$. Moreover, from (19), we have

$$\begin{aligned}
&\lim_{N_{SR^{(i)}},N_{R^{(i)}D}\to 0} P_{AF}(\gamma_{\text{th}}) \\
&= \prod_{i=1}^{N_r}\left(1-\left(1+\frac{d_{SR}^{(i)}\gamma_{\text{th}}}{\left(a_{SR}^{(i)}-\gamma_{\text{th}}c_{SR}^{(i)}\right)}\right)^{-1}\left(1+\frac{d_{RD}^{(i)}\gamma_{\text{th}}}{\left(a_{RD}^{(i)}-\gamma_{\text{th}}c_{RD}^{(i)}\right)}\right)^{-1}\right) \\
&\simeq \prod_{i=1}^{N_r}\left(1-e^{-\frac{d_{SR}^{(i)}\gamma_{\text{th}}}{a_{SR}^{(i)}}\left(1+\frac{c_{SR}^{(i)}\gamma_{\text{th}}}{a_{SR}^{(i)}}\right)-\frac{d_{RD}^{(i)}\gamma_{\text{th}}}{a_{RD}^{(i)}}\left(1+\frac{c_{RD}^{(i)}\gamma_{\text{th}}}{a_{RD}^{(i)}}\right)}\right) \qquad (33) \\
&= \prod_{i=1}^{N_r}\left(1-e^{-\left(\left|\frac{\nu_{R^{(i)}}^{r}}{\mu_{R^{(i)}}^{r}}\right|^2+\left|\frac{\nu_{D}^{r}}{\mu_{D}^{r}}\right|^2\right)\gamma_{\text{th}}-\left(\left|\frac{\nu_{S}^{t}}{\mu_{S}^{t}}\right|^2\left|\frac{\nu_{R^{(i)}}^{r}}{\mu_{R^{(i)}}^{r}}\right|^2+\left|\frac{\nu_{D}^{r}}{\mu_{D}^{r}}\right|^2\left|\frac{\nu_{R^{(i)}}^{t}}{\mu_{R^{(i)}}^{t}}\right|^2\right)\gamma_{\text{th}}^2}\right),
\end{aligned}$$

Defining $\alpha_i \triangleq \left|\frac{\nu_{R^{(i)}}^{r}}{\mu_{R^{(i)}}^{r}}\right|^2+\left|\frac{\nu_{D}^{r}}{\mu_{D}^{r}}\right|^2$ and $\beta_i \triangleq \left|\frac{\nu_{S}^{t}}{\mu_{S}^{t}}\right|^2\left|\frac{\nu_{R^{(i)}}^{r}}{\mu_{R^{(i)}}^{r}}\right|^2+\left|\frac{\nu_{D}^{r}}{\mu_{D}^{r}}\right|^2\left|\frac{\nu_{R^{(i)}}^{t}}{\mu_{R^{(i)}}^{t}}\right|^2$ and expanding the exponential product, Eqn. (33) can be expressed as follows

$$\begin{aligned}
&\lim_{N_{SR^{(i)}},N_{R^{(i)}D}\to 0} P_{AF}(\gamma_{\text{th}}) = \\
&\quad 1+\sum_{k=1}^{N_r}(-1)^k\sum_{n=1}^{\binom{N_r}{k}} e^{-\left(\sum_{j=1}^{k}\phi_{k,n,j}\right)\gamma_{\text{th}}-\left(\sum_{j=1}^{k}\theta_{k,n,j}\right)\gamma_{\text{th}}^2}, \qquad (34)
\end{aligned}$$

where $\phi_{k,n,j}$ and $\theta_{k,n,j}$ are the j^{th} elements of the n^{th} subsets, each comprised of k elements of the sets $\{\alpha_1,\ \alpha_2,\ \ldots,\ \alpha_{N_r}\}$ and $\{\beta_1,\ \beta_2,\ \ldots,\ \beta_{N_r}\}$, respectively. It is worth mentioning that $k \in \{1,\ \ldots, N_r\}$, $n \in \left\{1,\ \ldots,\ \binom{N_r}{k}\right\}$, and $j \in \{1,\ \ldots,\ k\}$. For more details on the exponential product expansion, please refer to a more detailed example provided in [29].

From (32) and (34) and evaluating the integral in (31), we get Eqn. (35), given at the top of the next page, where $\Gamma_{k,n}=\sum_{j=1}^{k}\phi_{k,n,j}$, $\Psi_{k,n}=\sum_{j=1}^{k}\theta_{k,n,j}$, and $\text{erf}(.)$ is the integral representation of the error function in [30, Eqn. 8.251.1]. Although the asymptotic outage probability expression in Eqn. (35) is complicated, considering the special case of interest where all nodes suffer from the same IQI levels results in the following compact expression

$$\begin{aligned}
P_{SRD}^{(MRC)} \doteq \left|\frac{\nu}{\mu}\right|^2\gamma_{\text{th}}+\sqrt{\frac{\pi}{8}}\sum_{k=1}^{N_r}\frac{(-1)^{k+1}}{\sqrt{k}}\binom{N_r}{k}e^{\frac{k}{2}} \\
\left(\text{erf}\left[\frac{k}{2}\right]-\text{erf}\left[\sqrt{\frac{k}{2}}\left(2\left|\frac{\nu}{\mu}\right|^2\gamma_{\text{th}}+1\right)\right]\right). \qquad (36)
\end{aligned}$$

Though Eqn. (36) represents a special case, it is still difficult to gain insights into the functional dependence of the asymptotic outage probability on $\left|\frac{\nu}{\mu}\right|^2$ and γ_{th}. However, it turns out that such an insight can be gained by differentiating (36) with respect to $\left|\frac{\nu}{\mu}\right|^2$, which we denote by ζ, assuming that the remaining parameters are fixed, to get

$$\begin{aligned}
\frac{\partial P_{SRD}^{(MRC)}}{\partial\zeta} &\doteq \gamma_{\text{th}}\left[1+\sum_{k=1}^{N_r}(-1)^k\binom{N_r}{k}e^{-k\left(2\zeta^2\gamma_{\text{th}}^2+2\zeta\gamma_{\text{th}}\right)}\right] \\
&\doteq \begin{cases}\gamma_{\text{th}}\left[1-e^{-2\zeta\gamma_{\text{th}}(\zeta\gamma_{\text{th}}+1)}\right]^{N_r}, & \zeta\le\frac{1}{\gamma_{\text{th}}} \\ 0, & \zeta>\frac{1}{\gamma_{\text{th}}}\end{cases} \qquad (37)
\end{aligned}$$

For IQI levels and transmission rate that satisfy the condition $\zeta\gamma_{\text{th}} = \left|\frac{\nu}{\mu}\right|^2(2^{r_{\text{th}}}-1) << 1$, Eqn. (37) can be further simplified as follows

$$\left.\frac{\partial P_{SRD}^{(MRC)}}{\partial\zeta}\right|_{\zeta\gamma_{\text{th}}<<1} \simeq (2\zeta)^{N_r}(\gamma_{\text{th}})^{N_r+1}. \qquad (38)$$

From (38), it is clear that, at a fixed N_r and γ_{th}, the functional dependence of the asymptotic outage probability on the IQI level can be accurately approximated as follows

$$P_{SRD}^{(MRC)}\Big|_{\zeta\gamma_{\text{th}}<<1} \doteq \frac{2^{N_r}}{N_r+1}\left(\left|\frac{\nu}{\mu}\right|^2(2^{r_{\text{th}}}-1)\right)^{N_r+1}+\mathcal{C}, \qquad (39)$$

where $\mathcal{C}$ is a constant which does not depend on the IQI level. From this simple, yet accurate approximation as it will be verified in Section IV, it is clear that the asymptotic outage probability floor for AF OR with DRL decreases at an exponential rate of (N_r+1), at a fixed rate γ_{th}. Comparing the asymptotic outage probability floor expressions of AF OR both with and without DRL, which are proportional to $\left|\frac{\nu}{\mu}\right|^{2N_r+2}$ and $\left|\frac{\nu}{\mu}\right|^{N_r}$, respectively, quantifies the diversity gain of the DRL and its role in enhancing the system's robustness against IQI[4].

C. *Connections to DF Opportunistic Relaying*

Although DF OR relaying is beyond the scope of this paper, the interested readers are referred to [31] and the references therein, it is worth mentioning that similar analysis procedures to those in Sections III-B1, III-B2, and III-B3 can be applied to derive its outage probability.

1) With Direct Link and SC at the Destination: In SC, the destination selects either the DRL or the best relay link as shown in Section III-B2. Moreover, since we approximated the relay end-to-end instantaneous SINR of each relay as in (9), which is also the equivalent instantaneous SINR for the DF OR case [27], the end-to-end outage probability of DF OR with SC at D can be approximated as in (25). Furthermore, for no DRL, deriving the outage probability of DF OR follows exactly the same procedure as in Section III-B1 for AF OR.

2) With Direct Link and MRC at the Destination: Applying MRC at D results in a different outage probability definition as in [31, Eqn. (3a)] which showed that there is a correlation between the SINR of the $S\to R_*$ and $R_*\to D$ links even if the individual channel links are independent. This significantly complicates the outage probability analysis and introducing IQI makes it even more complicated! Although we have derived the analytical outage probability

[4]Analogous conclusions can be drawn about the impact of γ_{th} on the asymptotic outage probability for a given fixed IQI level and number of relays.

$$P_{SRD}^{(MRC)} \doteq \frac{d_{SD}}{a_{SD}}\left(\gamma_{\text{th}} - \tau_{SD}\gamma_{\text{th}}^2\right) + \frac{d_{SD}}{a_{SD}}\sum_{k=1}^{N_r}(-1)^k \sum_{n=1}^{\binom{N_r}{k}} \frac{1}{2\sqrt{\Gamma_{k,n}^3}} e^{-\gamma_{\text{th}}(\gamma_{\text{th}}\Gamma_{k,n}+\Psi_{k,n})}$$
$$\times \left(2\sqrt{\Gamma_{k,n}}\tau_{SD}\left(e^{\gamma_{\text{th}}(\gamma_{\text{th}}\Gamma_{k,n}+\Psi_{k,n})} - 1\right) + \sqrt{\pi} e^{\frac{\left(2\Gamma_{k,n}\gamma_{\text{th}}+\Psi_{k,n}\right)^2}{4\Gamma_{k,n}}}\right.$$
$$\left. \times \left(\tau_{SD}\Psi_{k,n} + (2\tau_{SD}\gamma_{\text{th}} - 1)\Gamma_{k,n}\right)\left(\text{erf}\left[\frac{\Psi_{k,n}}{2\sqrt{\Gamma_{k,n}}}\right] - \text{erf}\left[\frac{2\gamma_{\text{th}}\Gamma_{k,n} + \Psi_{k,n}}{2\sqrt{\Gamma_{k,n}}}\right]\right)\right) \quad (35)$$

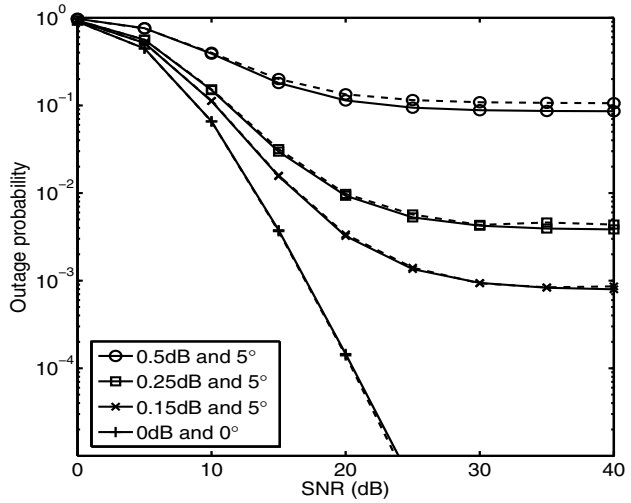

Fig. 3. Analytical (solid lines) and simulated (dashed lines) AF OR outage probabilities for different IQI levels, for $N_r = 3$ relays, $d_1 = 0.5$, $r_{\text{th}} = 4$ bps/Hz, and assuming no DRL.

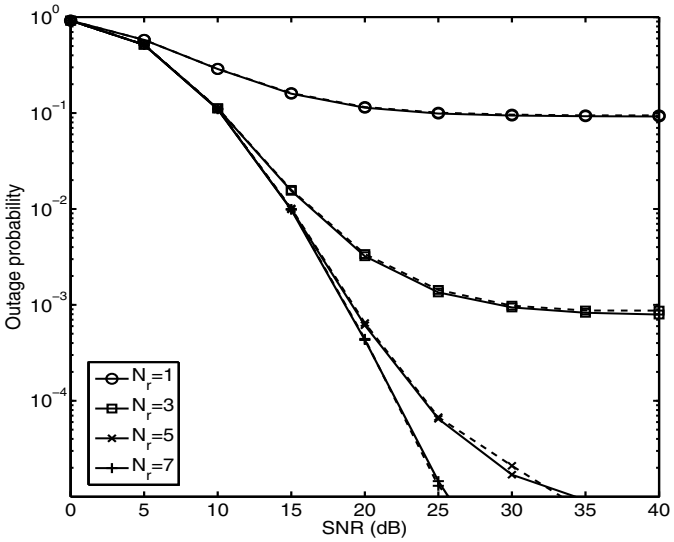

Fig. 4. Analytical (solid lines) and simulated (dashed lines) AF OR outage probabilities for amplitude imbalance of 0.15 dB, phase imbalance of 5°, $r_{\text{th}} = 4$ bps/Hz, and assuming no DRL.

expressions for this scenario, we did not include them in this paper due to space limitation and because it is not possible to simplify them to gain useful engineering insights.

IV. Numerical and Simulation Results

In this section, we present Monte-Carlo simulation results to demonstrate the accuracy of the outage probability expressions derived in Section III. Although our analytical expressions are for a general AF OR network layout and IQI levels, we consider the following special but insightful scenario where, unless otherwise stated, we assume three relays located on the perpendicular line midway between the S and D nodes and we denote the distance between this line and the S node by d_1. In addition, the distance between the S and D nodes is normalized to $d_{SD} = 1$; meanwhile, the distance between each pair of consecutive relays on the line is $d_{SD}/2$.

The CIR between any two nodes is generated using $L = 8$ uncorrelated zero-mean complex Gaussian taps with uniform power-delay profile and the variance of each tap is assumed to be $\frac{d_{IJ}^{-\xi}}{L}$, where ξ is set to 3.7. The S and R nodes transmit at the same power level, $\eta_0 = \eta_i = 1$; hence, $N_{SR^{(i)}} = N_{R^{(i)}D} = \frac{1}{SNR}$, $\forall\, i$. Finally, the number of OFDM subcarriers is 64 and the subcarrier index of interest is 15.

In Fig. 3, we assume that $d_1 = 0.5$, i.e. the relays lie on the perpendicular bisector between S and D. Therefore, the second relay lies on the line connecting the S and D nodes, while the other two relays form isosceles triangles with them. Moreover, all nodes suffer from the same IQI level, i.e. $(\mu_S^t)^* = \mu_D^r = \mu_{R^{(i)}}^r = \left(\mu_{R^{(i)}}^t\right)^*$ and $\nu_S^t = \nu_D^r = \nu_{R^{(i)}}^r = \nu_{R^{(i)}}^r\ \forall\ i$. Fig. 3 depicts the AF OR without DRL outage probabilities for different IQI levels at $r_{\text{th}} = 4$ bps/Hz and it shows the accuracy of the derived expression in (19). The outage probability simulations and analytical expressions coincide over the entire SNR range for different IQI levels. Moreover, Eqn. (22) accurately predicts the outage probability floor and quantifies its dependence on the IQI level, signal constellation size and number of relays.

Fig. 4 shows the impact of the number of relays on the outage probability floor for $d_1 = 0.5$ assuming no DRL between the S and D nodes when all nodes are impaired by the same IQI level of $10\log_{10}(1+\epsilon^{t/r}) = 0.15$ dB amplitude imbalance and $\theta^{t/r} = 5°$ phase imbalance. At low SNR (below 10 dB), there is no performance improvement due to any additional relay (beyond $N_r = 3$) because its path loss is greater than the existing relays' path losses, and hence, it is less likely to be selected. On the other hand, at high SNR (above 30 dB) and as shown by Eqn. (22), the outage probability floor is independent of path loss and the relays' positions while it is directly proportional to $\left|\frac{\nu}{\mu}\right|^{2N_r}$. With seven relays, the outage probability floor is almost eliminated for the considered SNR range.

For further assessment of the derived expressions for AF OR without DRL, we show in Fig. 5 the outage probabilities for a different scenario where the S and D nodes suffer from the same IQI level with amplitude and phase imbalances of

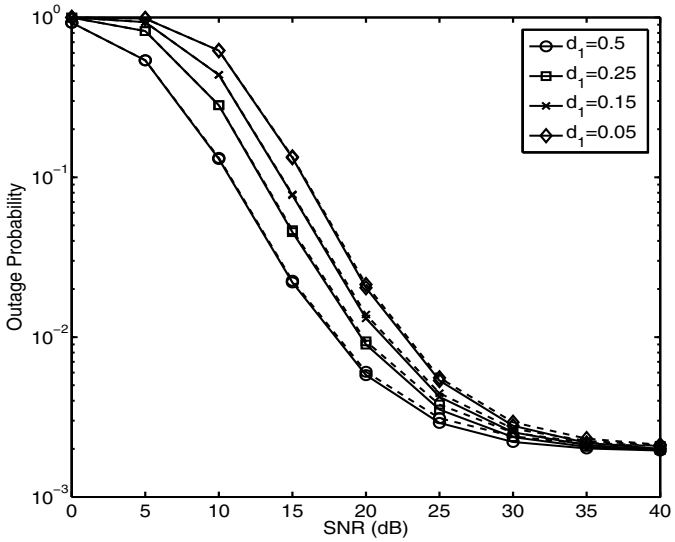

Fig. 5. Analytical and simulated AF OR outage probabilities for amplitude imbalance of 0.15 dB, phase imbalance of 5°, $r_{\text{th}} = 4$ bps/Hz, and assuming no DRL.

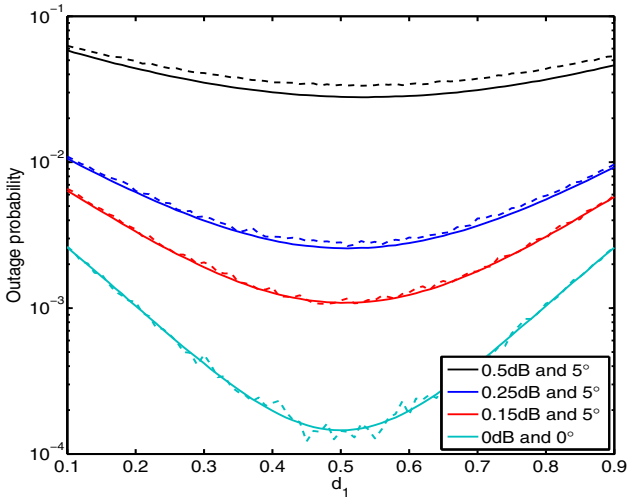

Fig. 6. Analytical and simulated AF OR outage probabilities with SNR=20 dB, $r_{\text{th}} = 4$ bps/Hz, and assuming no DRL.

0.25 dB and 5°, respectively, while the three relays are IQI-impaired with the same phase imbalance of 5° and amplitude imbalances of 0.1, 0.15, and 0.2 dB. This figure confirms the accuracy of the derived expressions even when the nodes suffer from different IQI levels and the relays are not at an equal distance from the S and D nodes. Furthermore, it is worth mentioning that the outage probability floor is independent of the channel gain, which depends on the relative distances between the relays and the S and D nodes, since the channel gain scales the signal and the interference power levels by the same amount.

In Fig. 6 we assume that the nodes involved in the first time slot transmissions are IQI-free while those involved in the second time slot transmissions are IQI-impaired. In other words, the source is IQI-free, the relays have IQI-free receiving RF front-ends and IQI-impaired transmitting RF front-ends, and the D node suffers from IQI. This implicitly assumes that the relays use different RF front-ends for receiving and transmitting where the former is IQI-free while the latter is IQI-impaired. Although this is not a practical assumption since the relays use the same RF front-end for both transmitting and

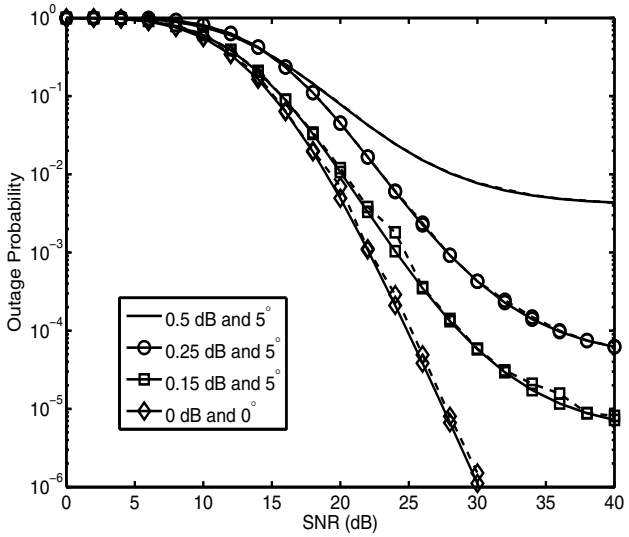

Fig. 7. Analytical (solid lines) and simulated (dashed lines) AF OR outage probabilities for different IQI levels, for $N_r = 3$ relays, $d_1 = 0.5$, $r_{\text{th}} = 4$ bps/Hz and assuming DRL with SC at the D node.

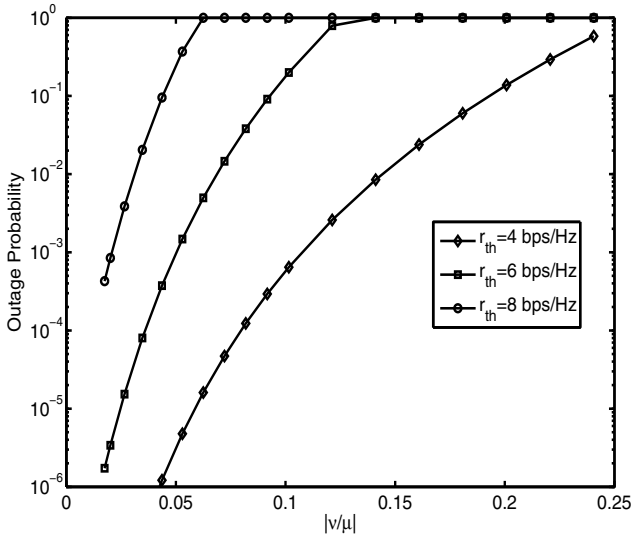

Fig. 8. Analytical outage probability (solid lines) and simulated outage probability (dashed lines) versus IQI leakage and $\theta = 2^o$ for AF OR with SC and assuming SNR = 40 dB.

receiving, we make this assumption to validate our outage expressions for different scenarios. Moreover, we assume the same IQI level at the relays and the destination nodes. As shown in Fig. 6, the simulations and the analytical expressions coincide over the whole range of d_1. It is well-known that the best position for the relays is to be midway between the S and D nodes for the IQI-free scenario [32]. Interestingly, Fig. 6 demonstrates that this is still the best position even if the nodes suffer from IQI. However, as the IQI level increases, the sensitivity of the outage probability to the exact relay location decreases since it becomes dominated by IQI effects.

Figures 3 to 6 assume no DRL, while in Figures 7 and 8 we assume the AF OR protocol with DRL and SC at the D node. We plot the outage probability versus the SNR and the IQI leakage levels which is $\left|\frac{\nu}{\mu}\right|$, respectively, for the special case of interest described at the beginning of this section.

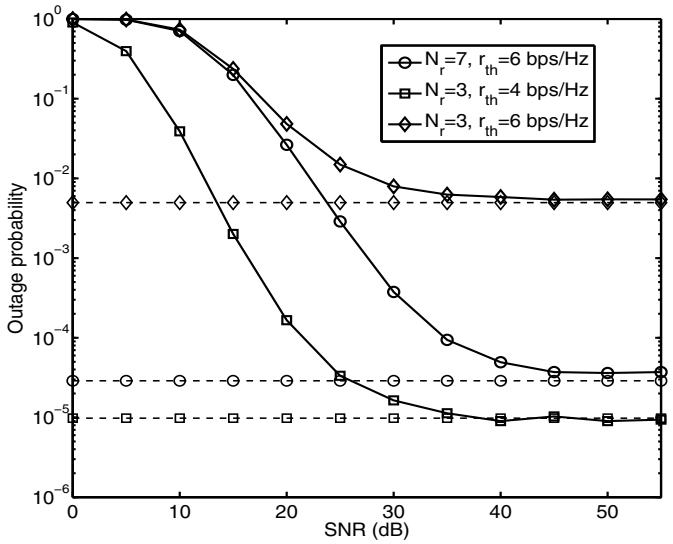

Fig. 9. AF OR analytical outage probability floor (dashed lines) and simulated outage probability (solid lines) for different IQI levels, with DRL and MRC at the D node.

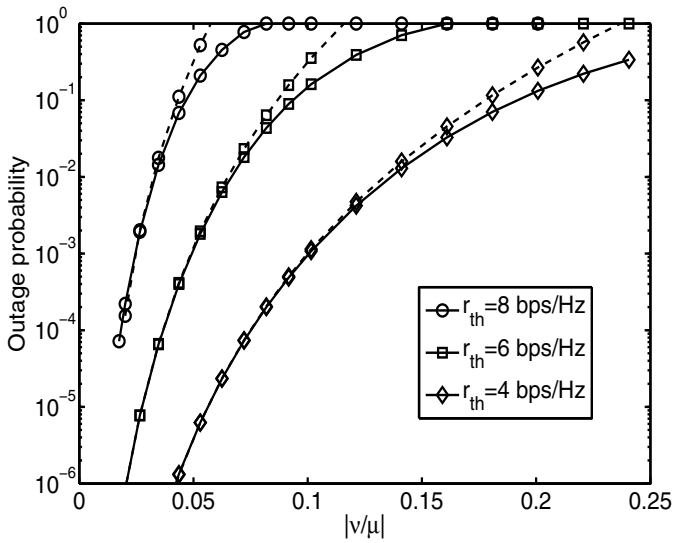

Fig. 10. Asymptotic analytical outage probability (solid lines) and its approximation (dashed lines), in Eqn. (39), versus IQI leakage for $\theta = 2^{\circ}$, for AF OR scheme with DRL and MRC at the D node.

The outage probability simulations and analytical expressions coincide over the entire range of SNR. Furthermore, Eqn. (26) accurately illustrates the outage probability functional dependence on the IQI level, input SNR, and number of relays.

Figures 9 and 10 depict the AF OR outage probability in the presence of the DRL and assuming ideal MRC at the D node. Moreover, all the relays are assumed to lie on the perpendicular bisector between the S and D nodes with $d_1 = 0.5$. Specifically, Fig. 9 illustrates the accuracy of the outage probability floor expression derived in Eqn. (36) in Section III-B3 for two simulation scenarios. The circle and diamond markers refer to the first scenario where all nodes suffer from the same IQI level with amplitude and phase imbalances of 0.15 dB and 5°, respectively. The second scenario is represented by square markers where all nodes are impaired with the same phase imbalance of 5° and different amplitude imbalance levels. The S and D nodes' amplitude imbalances are 0.2 dB and 0.15 dB, respectively, while those of the relays are (0.1 dB, 0.15 dB), (0.15 dB, 0.2 dB), and (0.2 dB, 0.3 dB) where the first and second elements of each pair are the transmit and receive amplitude imbalances, respectively, of each relay node. Fig. 10 shows the outage probability versus the IQI leakage level, $\left|\frac{\nu}{\mu}\right|$, at SNR = 40 dB assuming three relays on the perpendicular line midway between the S and D nodes. This figure clearly demonstrates how increasing the IQI level severely degrades the outage performance especially for bigger signal constellations. Moreover, it confirms the valid range of our asymptotic outage probability floor approximation in Eqn. (39), which is governed by the condition $\left|\frac{\nu}{\mu}\right|^2 (2^{r_{\text{th}}} - 1) << 1$. As shown in the figure, this condition is satisfied over practical outage probability levels, less than 10^{-2}, which reaffirms the insights discussed in Section III-B3 and their value in designing practical communication systems.

Finally, Fig. 11 depicts the outage probability versus the IQI leakage level for AF OR with and without DRL in the high-SNR regime ($SNR = 40$ dB) for the special case of interest where all nodes suffer from the same IQI level, $r_{th} = 6$ bps/Hz, $\theta = 2^o$, and the three relays lie on the perpendicular bisector between the S and D nodes. As shown in Fig. 11, performing MRC at the D node in the presence of a DRL results in a lower outage probability and more robustness against IQI than SC. We conclude by noting that Fig. 11 also demonstrates that performing either SC or MRC at the D node in the presence of a DRL achieves lower outage than the case of no DRL which matches our with our asymptotic analysis in Section III.

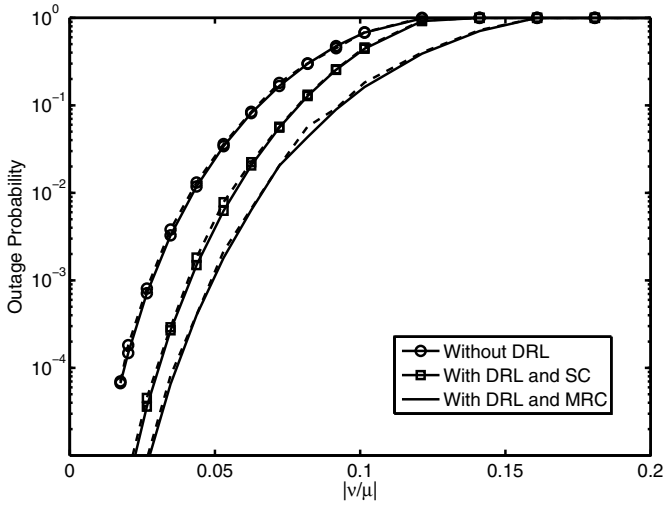

Fig. 11. AF asymptotic analytical outage probability (solid lines) and simulated outage probability (dashed lines) with/without DRL probability versus IQI leakage level, $r_{th} = 6$ bps/Hz, $\theta = 2^o$ and SNR=40 dB.

V. Conclusions

In this paper, we studied the outage performance of OFDM opportunistic relaying, both with and without direct link, in the presence of IQI in all nodes. We derived an accurate approximation for the outage probability for the general case where each node suffers from a different IQI level and without restricting the distance between the source and the relay to be the same for all relays. Our simulations demonstrated the accuracy of the derived analytical expressions and illustrated that the detrimental IQI effects on outage can be significantly

reduced using only few opportunistic relays. Furthermore, we considered a special but insightful scenario where there is no direct link, all nodes suffer from the same IQI level and the relay nodes lie on the perpendicular bisector between the S and D nodes. In this case, we showed that the outage probability floor is proportional to the product of the signal constellation size and the IQI interference to signal ratio raised to a power equal to the number of relays. Finally, we demonstrated that AF OR with direct link and ideal MRC at the D node has a higher tolerance to IQI effects compared to AF OR with direct link and SC at D node or AF without direct link.

REFERENCES

[1] K. Loa, C.-C. Wu, S.-T. Sheu, Y. Yuan, M. Chion, D. Huo, and L. Xu, "IMT-advanced relay standards [WiMAX/LTE Update]," *IEEE Commun. Mag.*, vol. 48, no. 8, pp. 40–48, 2010.

[2] C. Hoymann, W. Chen, J. Montojo, A. Golitschek, C. Koutsimanis, and X. Shen, "Relaying operation in 3GPP LTE: challenges and solutions," *IEEE Commun. Mag.*, vol. 50, no. 2, pp. 156–162, 2012.

[3] M. Fareed and M. Uysal, "On relay selection for decode-and-forward relaying," *IEEE Trans. Wireless Commun.*, vol. 8, no. 7, pp. 3341–3346, 2009.

[4] Y. Zhao, R. Adve, and T. J. Lim, "Improving amplify-and-forward relay networks: optimal power allocation versus selection," *IEEE Trans. Wireless Commun.*, vol. 6, no. 8, pp. 3114–3123, 2007.

[5] V. Shah, N. B. Mehta, and R. Yim, "Relay selection and data transmission throughput tradeoff in cooperative systems," in *Proc. 2009 IEEE Global Telecommunications Conference*, pp. 1–6.

[6] Y. Song, H. Shin, and E.-K. Hong, "MIMO cooperative diversity with scalar-gain amplify-and-forward relaying," *IEEE Trans. Commun.*, vol. 57, no. 7, pp. 1932–1938, 2009.

[7] A. Bletsas, H. Shin, and M. Z. Win, "Cooperative communications with outage-optimal opportunistic relaying," *IEEE Trans. Wireless Commun.*, vol. 6, no. 9, pp. 3450–3460, 2007.

[8] D. S. Michalopoulos, N. D. Chatzidiamantis, R. Schober, and G. K. Karagiannidis, "The diversity potential of relay selection with practical channel estimation," *IEEE Trans. Wireless Commun.*, vol. 12, no. 2, pp. 481–493, 2013.

[9] M. Dohler and Y. Li, *Cooperative Communications: Hardware, Channel and PHY*. Wiley, 2010.

[10] P. Banelli, G. Baruffa, and S. Cacopardi, "Effects of HPA nonlinearity on frequency multiplexed OFDM signals," *IEEE Trans. Broadcast.*, vol. 47, no. 2, pp. 123–136, 2001.

[11] N. W. Bikhazi and M. A. Jensen, "Impact of coupling on multiple-antenna capacity in correlated fast-fading environments," *IEEE Trans. Veh. Technol.*, vol. 58, no. 3, pp. 1595–1597, 2009.

[12] J. Qi, S. Aissa, and M.-S. Alouini, "Analysis and compensation of I/Q imbalance in amplify-and-forward cooperative systems," in *Proc. 2012 IEEE Wireless Comm. and Networking Conference*, pp. 215–220.

[13] P. Rabiei, W. Namgoong, and N. Al-Dhahir, "On the performance of OFDM-based amplify-and-forward relay networks in the presence of phase noise," *IEEE Trans. Commun.*, vol. 59, no. 5, pp. 1458–1466, 2011.

[14] T. Schenk, *RF Imperfections in High-Rate Wireless Systems*. Springer, 2008.

[15] M. Mokhtar, A. Gomaa, and N. Al-Dhahir, "OFDM AF relaying under I/Q imbalance: performance analysis and baseband compensation," *IEEE Trans. Commun.*, vol. 61, no. 4, pp. 1304–1313, 2013.

[16] M. Mokhtar, A.-A. A. Boulogeorgos, G. K. Karagiannidis, and N. Al-Dhahir, "Dual-Hop OFDM opportunistic AF relaying under joint transmit/receive I/Q imbalance," in *Proc. 2013 IEEE Global Telecommunications Conference.*

[17] F. Raphel and S. M. Sameer, "A novel interim channel estimation technique for MIMO mimicking AF cooperative relay systems," in *Proc. 2012 National Conference on Communications*, pp. 1–5.

[18] T. C. Schenk, E. R. Fledderus, and P. F. Smulders, "Performance impact of IQ mismatch in direct-conversion MIMO OFDM transceivers," in *Proc. 2007 IEEE Radio and Wireless Symposium*, pp. 329–332.

[19] H.-G. Ryu, "Diversity effect of OFDM communication with IQ imbalance in the Rayleigh fading channel," in *Proc. 2010 International Conference on Comm. Software and Networks*, pp. 489–493.

[20] L. Ju-hu and W. Wei-ling, "Performance of MIMO-OFDM systems with phase noise at transmit and receive antennas," in *Proc. 2011 International Conference on Wireless Communications, Networking and Mobile Computing*, pp. 1–4.

[21] A. van Zelst and T. C. W. Schenk, "Implementation of a MIMO OFDM-based wireless LAN system," *IEEE Trans. Signal Process.*, vol. 52, no. 2, pp. 483–494, 2004.

[22] M. O. Hansna and M.-S. Alouini, "A performance study of dual-hop trasmissions with fixed gain relays," *IEEE Trans. Wireless Commun.*, vol. 3, no. 6, pp. 1963–1967, 2004.

[23] A. Tarighat, R. Bagheri, and A. Sayed, "Compensation schemes and performance analysis of IQ imbalances in OFDM receivers," *IEEE Trans. Signal Process.*, vol. 53, no. 8, pp. 3257–3268, Aug. 2005.

[24] K.-S. Hwang, Y.-C. K. , and M.-S. Alouini, "Performance analysis of incremental relaying with relay selection and adaptive modulation over non-identically distributed cooperative paths," in *Proc. 2008 IEEE International Symposium on Information Theory*, pp. 2678–2682.

[25] H. Stark and J. Woods, *Probability, Statistics, and Random processes for engineers*, 4th ed. Prentice Hall, 2012.

[26] J. Hu and N. C. Beaulieu, "Performance analysis of decode-and-forward relaying with selection combining," *IEEE Commun. Lett.*, vol. 11, no. 6, pp. 489–491, 2007.

[27] A. Bletsas, A. Khisti, D. P. Reed, and A. Lippman, "A simple cooperative diversity method based on network path selection," *IEEE J. Sel. Areas Commun.*, vol. 24, no. 3, pp. 659–672, 2006.

[28] P. A. Anghel and M. Kaveh, "Exact symbol error probability of a cooperative network in a Rayleigh-fading environment," *IEEE Trans. Wireless Commun.*, vol. 3, no. 5, pp. 1416–1421, 2004.

[29] D. S. Michalopoulos and G. K. Karagiannidis, "Performance analysis of single relay selection in Rayleigh fading," *IEEE Trans. Wireless Commun.*, vol. 7, no. 10, pp. 3718–3724, 2008.

[30] I. S. Gradshteyn and I. M. Ryzhik, *Table of Integrals, Series, and Products*, 6th ed. Academic Press, 2000.

[31] R. Nikjah and N. C. Beaulieu, "Exact closed-form expressions for the outage probability and ergodic capacity of decode-and-forward opportunistic relaying," in *Proc. 2009 IEEE Global Telecommunications Conference*, pp. 1–8.

[32] L. Fei, L. Qinghua, L. Tao, and Y. Guangxin, "Impact of relay location according to SER for amplify-and-forward cooperative communications," in *Proc. 2007 IEEE International Workshop on Anti-Counterfeiting, Security, Identification*, pp. 324–327.

Mohamed Mokhtar received BSc degree in electronics and communications engineering from Alexandria University, Egypt, in 2008 and the MSc from Nile University, Egypt, in 2010. He is currently working towards the Ph.D. degree at the University of Texas at Dallas, USA. His research interests include cooperative communication and RF impairments equalization at the baseband.

Alexandros-Apostolos A. Boulogeorgos (S'11) was born in Trikala, Greece. He obtained the Diploma Degree (five years) in electrical and computer engineering from the Aristotle University of Thessaloniki, Greece, in 2012. Since 2012, he has been working towards his Ph.D. degree at the Department of Electrical and Computer Engineering, Aristotle University of Thessaloniki. His current research interests include cooperative communications, RF impairments equalization and interference alignment.

George K. Karagiannidis For a current biography, please refer to p. 1645 in this issue.

Naofal Al-Dhahir For a current biography, please refer to IEEE TRANSACTIONS ON COMMUNICATIONS, vol. 61, no. 5, May 2013, p. 1925.